IOPscience iopscience.iop.org

Home Search Collections Journals About Contact us My IOPscience

Devitrification of the glassy state in suspensions of charged platelets

This article has been downloaded from IOPscience. Please scroll down to see the full text article.

2009 J. Phys.: Condens. Matter 21 474218

(http://iopscience.iop.org/0953-8984/21/47/474218)

View the table of contents for this issue, or go to the journal homepage for more

Download details:
IP Address: 129.252.86.83
The article was downloaded on 30/05/2010 at 06:07

Please note that terms and conditions apply.

J. Phys.: Condens. Matter **21** (2009) 474218 (7pp) doi:10.1088/0953-8984/21/47/474218

# Devitrification of the glassy state in suspensions of charged platelets

**M C D Mourad, A A Verhoeff, D V Byelov, A V Petukhov and H N W Lekkerkerker**

Van't Hoff Laboratory for Physical and Colloid Chemistry, Debye Institute, Utrecht University, Padualaan 8, 3584 CH Utrecht, The Netherlands

Received 17 April 2009, in final form 8 July 2009
Published 5 November 2009
Online at stacks.iop.org/JPhysCM/21/474218

**Abstract**

Colloidal suspensions of charged gibbsite platelets at salt concentrations of $10^{-2}$ M and below and with a sufficiently high particle concentration form a kinetically arrested, glassy state. We study the evolution of the glassy state in suspensions of three different gibbsite systems. Despite differences in size and polydispersity, we observe small, iridescent grains of the hexagonal columnar phase, for all these systems after periods of months to years. The connections between this devitrification phenomenon and the structure of the glassy state are discussed.

(Some figures in this article are in colour only in the electronic version)

## 1. Introduction

The mission statement of *Journal of Physics: Condensed Matter* reads: 'Reporting experimental and theoretical studies of the structural, thermal, mechanical, electrical, magnetic, optical and surface properties of condensed matter. Separate Surface, Interface and Atomic-Scale Science and Liquids, Soft Matter and Biological Physics sections keep the journal at the forefront of materials science and condensed matter physics'. The success in this mission is to a large measure due to the work of Richard Palmer as the Senior Publisher. Therefore it is a great pleasure to contribute with this paper to the special issue of *Journal of Physics: Condensed Matter* in honour of Richard Palmer.

This paper deals with the devitrification of the glassy state in dispersions of charged colloidal platelets. This subject is part of the field of 'Colloid Physics'. The *Journal of Physics: Condensed Matter* has played a highly significant role in establishing this field. The *Journal of Physics: Condensed Matter* became a forum for modern liquid state research and vital part of condensed matter physics, due to the formation of the Liquids and Soft Matter Board (now: Liquids, Soft Matter and Biological Physics). In addition, the highly professional publication of the proceedings of the triennial Liquid Matter Conference organized by the Liquids Section of the Condensed Matter Division of the European Physical Society, again under the direction of Richard Palmer, further strengthened this role.

In his classical (1905) paper on Brownian motion Einstein [1] clearly recognized that colloidal particles in a suspension obey the same thermo-statistics as atoms in assemblies. Hence, the thermodynamic properties of an assembly of colloids are formally the same as those of an assembly of atoms with an interatomic potential of the same form [2]. Conceptually, the simplest interaction between particles is that in a model system consisting of hard spheres, which experience an infinitely repulsive force when they touch, but no forces otherwise. Originally, this was proposed as a mathematically simple model of atomic liquids [3]. Over the last decades its benefit as a basic model for complex liquids has been demonstrated [2]. Although hard-sphere-interacting atoms do not exist, good approximations to hard-sphere-interacting colloids do [4, 5].

The equilibrium phase behaviour of systems of hard spheres was established many years ago by computer simulations [6, 7]. Up to a volume fraction $\varphi = 0.494$ the equilibrium state is a fluid, while for $\varphi > 0.545$ the equilibrium state is a crystal. For $0.494 < \varphi < 0.545$, the fluid and crystal states coexist. This phase behaviour has indeed been observed in concentrated suspensions of nearly hard-sphere-interacting colloids [4, 5].

Moreover, Pusey and Van Megen [5] observed that in disordered suspensions with volume fractions above 0.58, particles become so tightly trapped, or 'caged', by their neighbours that they are unable to move far enough to nucleate crystals. Instead, long-lived amorphous states called 'colloidal glasses' are obtained (for a recent review see [8]).

In 1999 Fabian *et al* [9] and Bergenholtz and Fuchs [10] considered the effect of the addition of short-ranged attraction

 © 2009 IOP Publishing Ltd Printed in the UK

to the hard-sphere repulsion between particles. They predicted a new scenario of transitions with a pocket of liquid and crystal states enclosed by a repulsive glass and an attractive glass. This remarkable prediction has been verified experimentally, using colloidal particles with a tunable depletion attraction induced by the addition of non-adsorbing polymer molecules [11–13].

Remarkably, a phase diagram with the sol-region enclosed by two different kinetically arrested states turned out to be typical, not only for spherical colloids, but also for anisometric colloids. In particular, in suspensions of natural and synthetic smectite clays a very similar situation is observed experimentally [14–17] and has been discussed theoretically [18]. Here, the balance between attractive and repulsive interactions is tuned by variation of the ionic strength. In these suspensions an attractive gel is observed at salt concentrations above $10^{-3}$–$10^{-2}$ M and a glass[1] is observed at $10^{-4}$–$10^{-5}$ M, while an enclosed region of sol states is found. Michot *et al* [16] observed isotropic–nematic phase equilibria in the sol-region.

Recently, we have observed that suspensions of charged colloidal gibbsite platelets—which may be considered as model clay particles—display similar sol–gel/glass behaviour [19, 20]. Birefringence and iridescence show that in the sol state both nematic and hexagonal columnar liquid crystal phases are formed. A decrease of the salt concentration and/or increase of the gibbsite concentration in the nematic phase gradually transforms from the discotic nematic ($N_D$) into the columnar nematic ($N_C$) with strong side-to-side interparticle correlations [21]. Subsequently, this $N_C$ phase shows a transition to the hexagonal columnar phase, although at high particle concentration this phase transition is preempted by the formation of a kinetically arrested state. Small angle x-ray scattering (SAXS) experiments show that the structural features of this arrested state are similar to those of the $N_C$ phase.

Here, we focus on the ageing of this kinetically arrested state of gibbsite suspensions just beyond the sol–gel transition, as schematically illustrated in figure 1. In all samples small hexagonal columnar crystallites are eventually (months–years) observed.

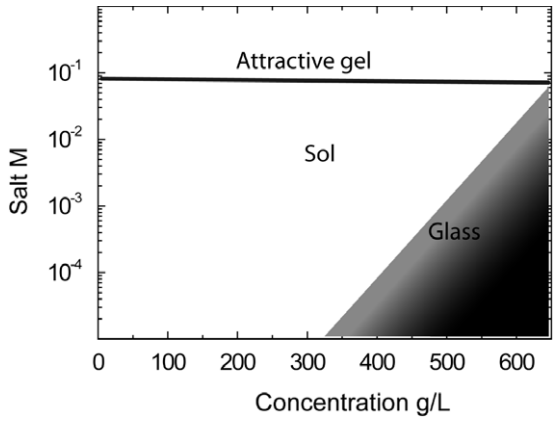


**Figure 1.** Schematic sol–gel/glass diagram of charged colloidal gibbsite platelets in water.

## 2. Experimental details

### *2.1. Particle preparation and characterization*

For this work we prepared three different systems of colloidal gibbsite platelets (A, B, and C). Each system was synthesized from an acidic aqueous solution containing hydrochloric acid (HCl 0.09 M, 37%, Merck), aluminium sec-butoxide (0.08 M, 95%, Fluka Chemika) and aluminium isopropoxide (0.08 M, 98+%, Acros Organics) [22]. The mixture was mechanically stirred for 10 days and subsequently heated in a glass reaction vessel in a water bath at 85 °C for 72 h. Next, the colloidal dispersions were centrifuged at 1200*g* (overnight, 15–20 h) in order to remove the smallest particles and decrease the polydispersity.

[1] This state is also commonly referred to as repulsive gel [14]. We will refer to it as a glass following [18] since the kinetic arrest originates from caging effects.

System A results from a single reaction step, while systems B and C were grown in a two-step procedure [23]. This involved redispersion of the platelets in the acidic aluminium alkoxide solution, as described above, and another heat treatment at 85 °C for 72 h. Before use the dispersions were dialyzed against demineralized water in tubes of regenerated cellulose (Visking, MWCO 12 000–14 000) until the conductivity dropped to 20 $\mu$S cm$^{-1}$. Moreover, aluminium chlorohydrate (0.6 g per gram gibbsite particles, Locron P, Hoechst AG, Germany) was added to the suspensions to hydrolyze and form $Al_{13}$ Keggin ions ($[Al_{13}O_4(OH)_{24}(H_2O)_{12}]^{7+}$) and thereby increase the stability of the gibbsite platelets [24]. The resulting suspensions were inspected with transmission electron microscopy (TEM). From the micrographs (see figure 2) the diameter of over 200 individual hexagonal particles was measured, from which the average diameter ($\langle D \rangle$) and the standard deviation ($\sigma_D$) were determined. The results are: system A $\langle D \rangle = 207$ nm with $\sigma_D = 35\%$, system B $\langle D \rangle = 270$ nm with $\sigma_D = 18\%$, and system C $\langle D \rangle = 205$ nm with $\sigma_D = 23\%$.

### *2.2. Sample preparation*

Concentrated gibbsite dispersions were prepared and set at ionic strength by centrifugation and redispersion in a NaCl solution in demineralized water. Samples for visual observation by the naked eye were put in large capillaries (1.0 mm × 10.0 mm cross section, Vitrotubes, VitroCom Inc.) that were then flame sealed. Polarization microscopy samples were prepared in 50 mm × 4 mm × 0.2 mm sized glass capillaries (VitroCom Inc.), which were then flame sealed and glued to avoid evaporation of the solvent. For x-ray experiments, samples were transferred into round Mark tubes (Quartz, 2 mm diameter and about 10 $\mu$m wall thickness, W Müller, Berlin, Germany).

### *2.3. Naked-eye and polarizing microscope observations*

Visual inspection was performed on a regular basis. For this, a home-built polarization setup was used, consisting of two crossed polarizing filters that could be illuminated by a 150 W

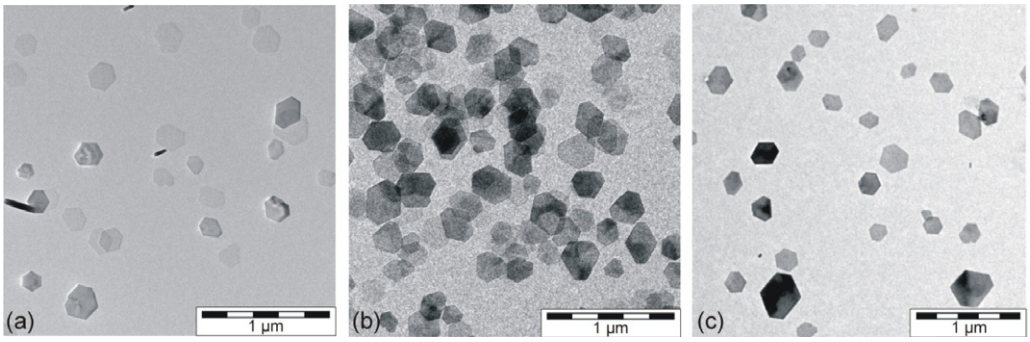


**Figure 2.** Transmission electron micrographs of the gibbsite platelets of systems A (panel (a)), B (panel (b)), and C (panel (c)).

lamp in combination with a condenser lens and a ground glass diffuser for homogeneous illumination. The samples in this polarization setup were photographed with a Nikon Coolpix 995 digital camera.

For investigation in more detail we used a Nikon LV100 Pol polarization microscope with 10× and 20× Nikon ELWD Plan Fluor objectives, and equipped with a QImaging MicroPublisher 5 megapixel CCD camera. Bragg reflections were observed with the polarization microscope while the sample was illuminated with a cold light source (Dolan Jenner, Model 190).

### *2.4. Small angle x-ray scattering*

X-ray studies were performed at the Dutch-Belgian beam line BM-26 DUBBLE of the European synchrotron radiation facility (ESRF) in Grenoble, France in September 2006 with 1 month old samples and in April 2008 using the same set of samples (20 months after preparation). We used our recently developed microradian x-ray diffraction setup, similar to the one described in the literature [25]. In brief, the x-ray beam was focused by a set of compound refractive lenses (CRL) [26] at the phosphor screen of the CCD (charge-coupled device) x-ray detector (Photonic Science, 4008 pixel × 2671 pixel of 22 $\mu$m$^2$). Any focusing of the beam before the experimental hutch was avoided to achieve the maximum transverse coherence length of the beam [25]. The capillaries were placed just after the CRLs at a distance of about 8 m from the detector. This setup allows an angular resolution of the order of 5–7 $\mu$rad to be achieved. X-ray photon energies of 13 keV (wavelength: $\lambda = 0.095$ nm) and 15 keV ($\lambda = 0.0825$ nm) were used in 2006 and 2008, respectively. The beam diameter in the sample was about 0.5 mm.

## 3. Results

We observed a transition from a sol state, displaying liquid crystal phase transitions, to a kinetically arrested state upon increase of the particle concentration in all three samples at salt concentrations of $10^{-2}$ M or lower. Below we present the observations of the optical and structural changes with time in these glassy states.

In figure 3 we present two samples of system A, one in the sol-region and one in the glassy state. The sample

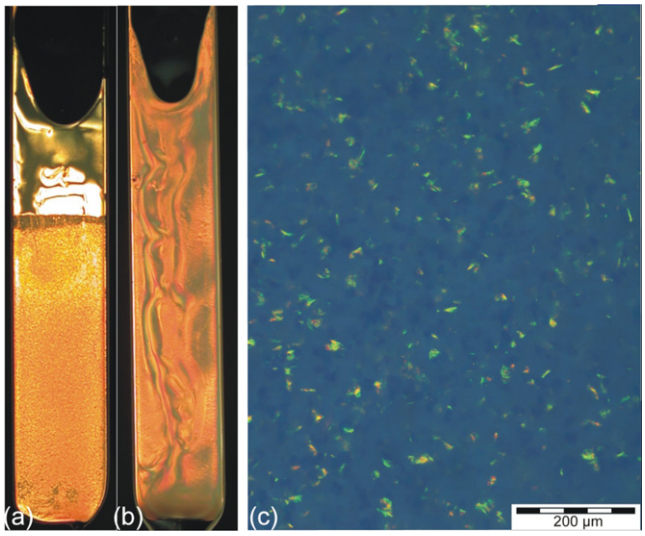


**Figure 3.** Samples of system A observed between crossed polarizers, at (a) 850 g l$^{-1}$ with nematic-hexagonal columnar phase coexistence and (b) at 1050 g l$^{-1}$ in the glassy state, both with $10^{-2}$ M NaCl. (c) Micrograph of the hexagonal columnar phase in (a) under white light illumination.

in the sol-region displays coexistence of the nematic and the hexagonal columnar phase, as is evident from the birefringent patterns and optical iridescence. The sample in the glassy state displays birefringent patterns that originate from the macroscopic orientational ordering caused by the shear forces during the filling of the capillary, but no iridescence.

The patterns in the glassy sample persist over months (see figures 4(a) and (b)). Eventually, after more than one year, an interface appears in the top part of the sample which separates an upper layer, containing isotropic and nematic domains, from the lower part of the sample. The latter retained the original birefringence patterns, albeit slightly compressed. Apparently, the compression of the glassy phase under the influence of gravity lowers the particle concentration in the upper part of the sample to such a degree that it allows the formation of both isotropic and nematic domains.

After three months, optical iridescence was observed in the glass, originating from grains with a size of about 5 $\mu$m (figure 5(a)), which is much smaller than the hexagonal columnar grain size in the phase separated sample in figure 3.


**Figure 4.** Time evolution of the glass state of system A, as observed between crossed polarizers.

Moreover, the Bragg reflections in the glass are predominantly blue, rather than green-yellow-orange in the hexagonal columnar phase, indicating smaller intercolumnar distances.

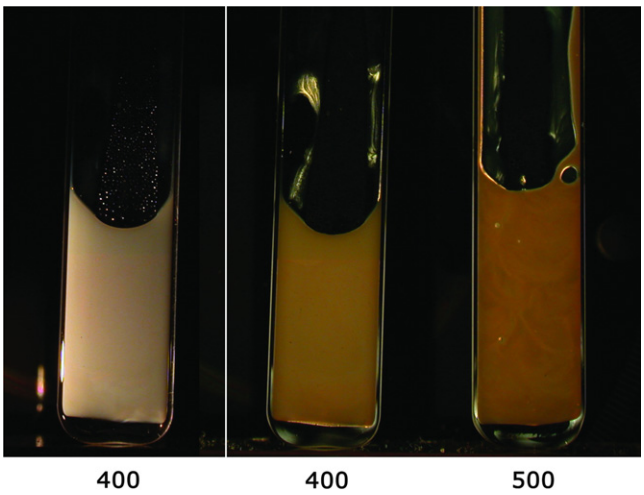


**Figure 6.** Samples of system B at $10^{-3}$ M NaCl added, observed under white illumination (400 g $l^{-1}$, left) and between crossed polarizers (400 g $l^{-1}$, middle, and 500 g $l^{-1}$, right). The sample at 400 g $l^{-1}$ displays isotropic–nematic phase coexistence, while the sample at 500 g $l^{-1}$ is in the glassy state.

After 17.5 months, the sizes and colours of the iridescent grains in the bottom part of the sample (figure 5(b)) are virtually unchanged (figure 5(a)). Towards the top of the sample, the grain size increases (figure 5(c)) and at the same time a shift of the Bragg colour from predominantly blue via green to orange is observed. Eventually, the iridescence resembles that of a hexagonal columnar phase (figure 5(d)).

In figure 6 we present two samples of system B, one in the sol-region and one in the glassy state. The sample in the sol-region displays an isotropic columnar phase coexistence (evident from the iridescence), with a sharp phase boundary. The sample in the glass state is birefringent. It has a sufficiently

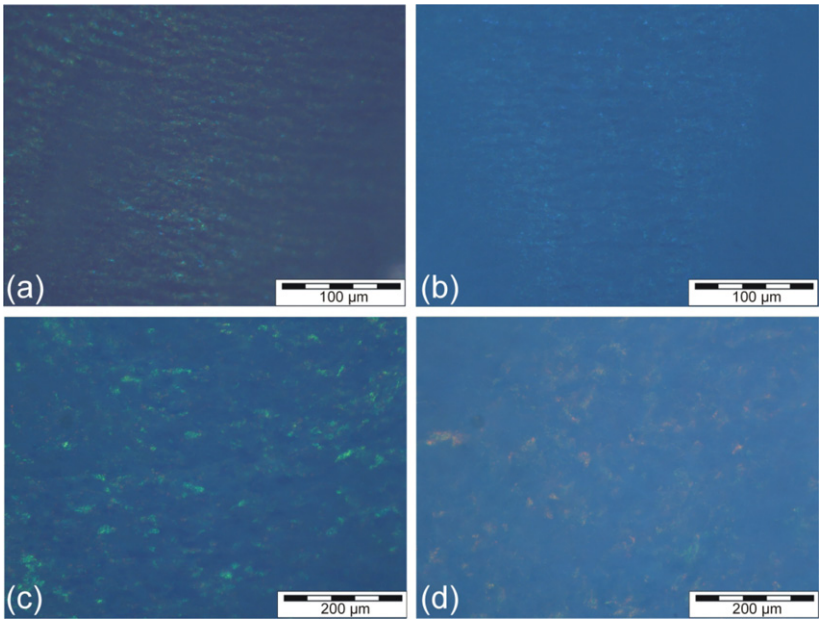


**Figure 5.** Micrographs of the glassy state of system A under illumination with white light; (a) bottom part after 3 months; (b) bottom part, (c) middle part, and (d) top part of the sample after 17.5 months.

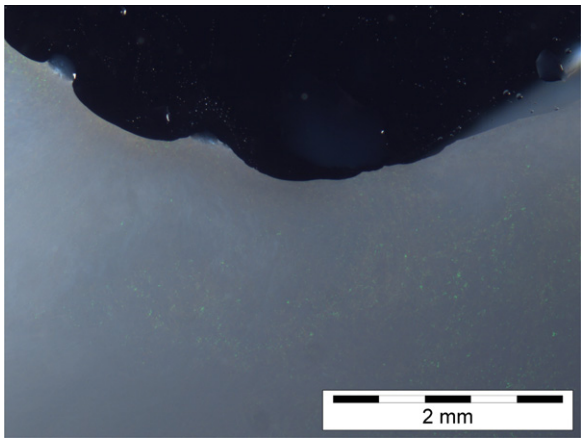


**Figure 7.** Iridescent grains in the top part of the sample of 500 g $l^{-1}$, system B at $10^{-3}$ M NaCl, observed 2 years after preparation.

high yield stress to trap air bubbles with a diameter of a few millimetres. The long term strength of this glass is reflected in the fact that even after two years there is no change in the outward appearance of the sample, including the position of the air bubble. Nevertheless, after two years iridescent grains with a size of about 15 $\mu$m are observed in the sample (figure 7). Despite the glass strength the platelets apparently still have enough free volume to locally rearrange into a hexagonal columnar arrangement.

In figure 8 we present two samples of system C, one in the sol-region (400 g $l^{-1}$) and one in the glassy state (500 g $l^{-1}$) at $10^{-2}$ M NaCl. The sample in the sol-region is completely birefringent with bright areas in the upper part. The brightness of the top layer may originate from a decreased turbidity in this part of the sample due to sedimentation, in combination with anchoring effects of the cell walls and the liquid–air interface on the orientation of the platelets. Eventually, after months, isotropic–nematic phase separation was observed in the top part of this sample. In order to study the structure of the sample in more detail in the glassy state and its eventual devitrification, we performed SAXS measurements one month and two years after preparation. The x-ray scattering pattern of the one month old sample (figure 9(a)) possesses a clear anisotropy. One can also see a pronounced broad peak at high $q$-region ($q_{001} = 0.194$ nm$^{-1}$) caused by the face-to-face correlations of platelets. The estimated face-to-face correlation distance is 32 nm. Moreover, there is a broad peak at the low $q$-region at $q_{100} = 0.030$ nm$^{-1}$ (figure 9(c)), which arises from side-to-side positional correlations of platelets with the correlation distance of $\frac{2\pi}{q_{100}}\frac{2}{\sqrt{3}} = 242$ nm, which is comparable to a diameter of particles obtained from TEM. The presence of pronounced side-to-side correlations points towards the $N_C$ structure, which is formed by stacks of platelets with nematic-like ordering among the stacks [21].

The SAXS pattern of the sample measured after two years (figure 9(b)) remains anisotropic and the face-to-face correlation distance remains almost the same 31 nm ($q_{001} = 0.206$ nm$^{-1}$) as for the one month old sample. However, the scattering at low $q$ changes significantly. The peak (at $q_{100} = 0.028$ nm$^{-1}$) becomes sharp and a second-order reflection peak


**Figure 8.** Samples of system C at $10^{-2}$ M NaCl between crossed polarizers (400 g $l^{-1}$, left and 500 g $l^{-1}$, right), 1 month after preparation. The sample at 400 g $l^{-1}$ displays the first signs of isotropic–nematic phase separation in the top of the sample, while the sample at 500 g $l^{-1}$ is in the glassy state.

appears at $q_{110} = 0.048$ nm$^{-1}$ (figure 9(b)). These $q$-values are related as $1{:}\sqrt{3}$ suggesting that reflections originate from the (100) and (110) Bragg reflections of the hexagonally arranged columns of platelets. These observations therefore demonstrate that in the course of two years hexagonal columnar domains have slowly developed within the glass state with $N_C$ structure.

## 4. Discussion and conclusions

The three gibbsite systems studied differ in particle size and particle polydispersity. The phase behaviour in the sol-region differs as well, though all three systems share the common feature that they enter a kinetically arrested state upon an increase of the particle concentration. After an ageing period, of months to years, this kinetically arrested state—while retaining its outside appearance—shows small iridescent grains, indicative of local transformation to the hexagonal columnar phase. While we do observe the effect of the shear-induced macroscopic orientational order on the orientation of the x-ray scattering patterns, we have no indication that the width of the scattering rings, and hence the degree of local columnar ordering, is affected by shear. Furthermore the length scale of the shear-induced macroscopic orientational ordering pattern (being of the size of the system) is much larger than the size of the hexagonal columnar nuclei. Hence

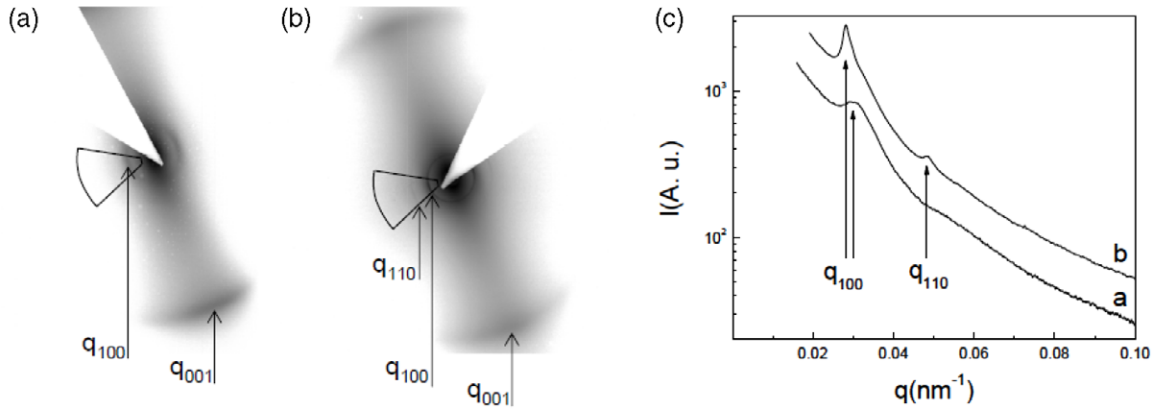


**Figure 9.** SAXS data of the system C at $10^{-2}$ M NaCl and 500 g $l^{-1}$ gibbsite concentration. 2D SAXS patterns collected one month after preparation (panel (a)) and two years after preparation (panel (b)) are displayed. Azimuthally integrated scattering profiles of the patterns shown in panels (a) and (b) are displayed in panel (c). The profiles were shifted in the vertical direction for better representation. The sector of integration is shown on panels (a) and (b).

it seems unlikely that shear directly affects the devitrification. Notwithstanding the large difference in polydispersity the three gibbsite systems exhibit the same devitrification phenomena. It is conceivable that nucleation of these crystallites is facilitated by the local columnar order in the preceding arrested state [20]. It may be instructive to compare our results to devitrification phenomena observed in molecular glasses. In these systems an unusual acceleration of the crystal growth rate below the glass transition has been ascribed [27, 28] to the slow beta mode [29], which is still active in the glassy state. Others ascribe it to the volume decrease upon ordering and the resulting creation of free volume near the interface between an ordered region and the surrounding glass region [30, 31].

The local transformation of the kinetically arrested columnar state to the hexagonal columnar phase is reminiscent of the dynamical heterogeneities observed in colloidal hard-sphere suspensions [32, 33]. A possible link between structural order and dynamic heterogeneity has been emphasized by Tanaka [34, 35]. These papers suggest that even in a supercooled liquid and a glassy state some degree of structural order may develop. If this is the case, it may act as an initiator for devitrification. Something similar seems to occur in our suspensions of platelike gibbsite colloids with the local columnar ordering playing the role of an initiator for devitrification. An alternative explanation may be that we are dealing with a nucleation phenomenon with a low nucleation barrier, which gives rise to many nuclei [36]. The low nucleation barrier may in turn be related to the columnar nature of the kinetically arrested state.

We want to conclude with a few comments on the relation between the glass state of a suspension of hard colloidal spheres and the glass state in a suspension of colloidal platelets. In the case of spheres, Frank [37] suggested, more than half a century ago, the existence of long-lived locally favoured structures, the geometry of which may prevent the system from relaxing to its equilibrium (crystal) state. Recently, Royall [38] provided direct experimental evidence of such a local structural mechanism for dynamical arrest. From this perspective, the hard-sphere fluid-to-crystal-transition may be considered as a locally favoured structure *avoiding* transition. In the case of platelets, computer simulations have shown that there is a strong tendency to form columns of platelets upon an increase of the volume fraction [39]. As the volume fraction is increased, these columns grow in length. The columns themselves are orientationally disordered and hence there is an appreciable interaction between different columns. It has been suggested, on the basis of small angle x-ray and neutron scattering on synthetic (Laponite [15]) and natural smectite (Montmorillonite [16, 17]) clays, and theoretical [18] considerations, that this interaction among the columns becomes so severe that it leads to a kinetically arrested glass phase. In our system of gibbsite platelets the particles are sufficiently monodisperse that the columns try to order in such a way that the packing problems are minimized. This then leads to a $N_C$ phase, and upon a further increase of the volume fraction to the hexagonal columnar phase. Clearly then, the locally favoured structures in the case of platelets do not, as such, prevent the formation of liquid crystal phases. However, above a limiting concentration the columns may become kinetically arrested, leading to a glassy state. The eventual observation of small crystallites in this case appears to be enabled, rather than obstructed, by locally favoured structures.

This is the opposite of the behaviour observed in the canonical hard-sphere model. In the case of platelets, the key structural element involved in the arrest transition is a stack of platelets, rather than an individual platelet. Such stacks are already present in the columnar nematic state, as well as in the arrested state itself. It may be that such (flexible) stacks can locally pack better in the arrested state than in the hexagonal columnar phase.

## Acknowledgments

The authors are grateful to Jeroen van Duijneveldt for his critical reading of the manuscript and several suggestions to improve its clarity.

Kristina Kvashnina, Esther van den Pol, Nicolas Vilayphiou, Dirk Detollenaere, Anatoly Snigirev and Wim Bras are thanked for their help in the SAXS experiments.

The Dutch Organization for Scientific Research (NWO) is thanked for the support of MCDM and for beam time at the DUBBLE beam line, ESRF (Grenoble). The work of AAV was supported by the Royal Netherlands Academy of Arts and Sciences (KNAW).

## References

[1] Einstein A 1905 On the motion, required by the molecular-kinetic theory of heat, of particles suspended in a fluid at rest *Ann. Phys.* **17** 549–60
[2] Pusey P N 1991 *Liquids, Freezing and Glass Transition* (*Les Houches Session 51, NATO Advanced Study Institute, Series B: Physics*) ed J P Hansen, D Levesque and J Zinn-Justin (Amsterdam: North-Holland) pp 763–942
[3] Hansen J P and McDonald I R 2006 *Theory of Simple Liquids* (London: Academic)
[4] de Kruif C G, Rouw P W, Jansen J W and Vrij A 1985 Hard sphere properties and crystalline packing of lyophilic silica colloids *J. Phys. Colloq.* **46** C3 295–308
[5] Pusey P N and van Megen W 1986 Phase behaviour of concentrated suspensions of nearly hard spheres *Nature* **320** 340–2
[6] Alder B J and Wainwright T A 1957 Phase transition for a hard sphere system *J. Chem. Phys.* **27** 1208–9
[7] Hoover W G and Ree F H 1968 Melting transition and communal entropy for hard spheres *J. Chem. Phys.* **49** 3609–17
[8] Pusey P N 2008 Colloidal glasses *J. Phys.: Condens. Matter* **20** 494202
[9] Fabbian L *et al* 1999 Ideal glass–glass transitions and logarithmic decay of correlations in a simple system *Phys. Rev.* E **59** R1347–50
[10] Bergenholtz J and Fuchs M 1999 Nonergodicity transitions in colloidal suspensions with attractive interactions *Phys. Rev.* E **59** 5706–15
[11] Eckert T and Bartsch E 2002 Re-entrant glass transition in a colloid–polymer mixture with depletion attractions *Phys. Rev. Lett.* **89** 125701
[12] Pham K N *et al* 2002 Multiple glassy states in a simple model system *Science* **296** 104–6
[13] Sciortino F 2002 Disordered materials—one liquid, two glasses *Nat. Mater.* **1** 145–6
[14] Abend S and Lagaly G 2000 Sol–gel transitions of sodium montmorillonite dispersions *Appl. Clay Sci.* **16** 201
[15] Levitz P *et al* 2000 Liquid–solid transition of Laponite suspensions at very low ionic strength: long range electrostatic stabilisation of anisotropic colloids *Europhys. Lett.* **49** 672–7
[16] Michot L J *et al* 2006 Liquid-crystalline aqueous clay suspensions *Proc. Natl Acad. Sci.* **103** 16101–4
[17] Shalkevich A *et al* 2007 Cluster, glass, and gel formation and viscoelastic phase separation in aqueous clay suspensions *Langmuir* **23** 3570–80
[18] Tanaka H, Meunier J and Bonn D 2004 Nonergodic states of charged colloidal suspensions: repulsive and attractive glasses and gels *Phys. Rev.* E **69** 031404
[19] Mourad M C D *et al* 2006 Gelation versus liquid crystal phase transitions in suspensions of plate-like particles *Phil. Trans. R. Soc.* A **364** 2807–16
[20] Mourad M C D *et al* 2008 Structure of the repulsive gel/glass in suspensions of charged colloidal platelets *J. Phys.: Condens. Matter* **20** 494201
[21] Mourad M C D *et al* 2009 Sol–gel transitions and liquid crystal phase transitions in concentrated aqueous suspensions of colloidal gibbsite platelets *J. Phys. Chem.* B **113** 11604–13
[22] Wierenga A M, Lenstra T A J and Philipse A P 1998 Aqueous dispersions of colloidal gibbsite platelets: synthesis, characterisation and intrinsic viscosity measurements *Colloids Surf.* A **134** 359–71
[23] Wijnhoven J E G J 2005 Seeded growth of monodisperse gibbsite platelets to adjustable sizes *J. Colloid Interface Sci.* **292** 403
[24] Hernandez J 1998 *Thèse de Doctorat de l'Université Pierre et Marie Curie* Université Pierre et Marie Curie, Paris, France
[25] Petukhov A V *et al* 2006 Microradian x-ray diffraction in colloidal photonic crystals *J. Appl. Crystallogr.* **39** 137–44
[26] Snigirev A *et al* 1996 A compound refractive lens for focusing high-energy x-rays *Nature* **384** 49
[27] Hikima T, Hanaya M and Oguni M 1999 Microscopic observation of a peculiar crystallization in the glass transition region and [beta]-process as potentially controlling the growth rate in triphenylethylene *J. Mol. Struct.* **479** 245–50
[28] Hatase M, Hanaya M and Oguni M 2004 Studies of homogeneous-nucleation-based crystal growth: significant role of phenyl ring in the structure formation *J. Non-Cryst. Solids* **333** 129–36
[29] Götze W 1991 Aspects of structural glass transitions *Liquids, Freezing and Glass Transition* (*Les Houches Session 51, NATO Advanced Study Institute, Series B: Physics*) ed J P Hansen, D Levesque and J Zinn-Justin (Amsterdam: North-Holland) pp 458–74
[30] Konishi T and Tanaka H 2007 Possible origin of enhanced crystal growth in a glass *Phys. Rev.* B **76** 220201
[31] Tanaka H 2003 Possible resolution of the Kauzmann paradox in supercooled liquids *Phys. Rev.* E **68** 011505
[32] Kegel W K and van Blaaderen A 2000 Direct observation of dynamical heterogeneities in colloidal hard-sphere suspensions *Science* **287** 290–3
[33] Weeks E R *et al* 2000 Three-dimensional direct imaging of structural relaxation near the colloidal glass transition *Science* **287** 627–31
[34] Tanaka H 1999 Two-order-parameter description of liquids. I. A general model of glass transition covering its strong to fragile limit *J. Chem. Phys.* **111** 3163–74
[35] Tanaka H 1999 Two-order-parameter description of liquids. II. Criteria for vitrification and predictions of our model *J. Chem. Phys.* **111** 3175–82
[36] Shi F G, Tong H Y and Ayers J D 1995 Free energy barrier to nucleation of amorphous-to-crystalline transformation selects the scale of microstructure of crystallized materials *Appl. Phys. Lett.* **67** 350–2
[37] Frank F C 952 Supercooling of liquids *Proc. R. Soc.* A **215** 43–6
[38] Royall C P *et al* 2008 Direct observation of a local structural mechanism for dynamic arrest *Nat. Mater.* **7** 556–61
[39] Veerman J A C and Frenkel D 1992 Phase behavior of disklike hard-core mesogens *Phys. Rev.* A **45** 5632–48